Integrated polarization beam splitter with relaxed fabrication tolerances

D. Pérez-Galacho,[1,*] R. Halir,[1] A. Ortega-Moñux,[1] C. Alonso-Ramos,[1] R. Zhang,[2] P. Runge,[2] K. Janiak,[2] H.-G. Bach,[2] A. G. Steffan,[3] and Í. Molina-Fernández[1]

[1]*Departamento de Ingeniería de Comunicaciones, ETSI Telecomunicación, Universidad de Málaga, 29010 Málaga, Spain*

[2]*Fraunhofer Institute for Telecommunications, Heinrich-Hertz-Institute, Einsteinufer 37, D-10587 Berlin, Germany*

[3]*u^2t Photonics AG, Reuchlinstr. 10/11, D-10553 Berlin, Germany*

[*]*diego.perez@ic.uma.es*

Abstract: Polarization handling is a key requirement for the next generation of photonic integrated circuits (PICs). Integrated polarization beam splitters (PBS) are central elements for polarization management, but their use in PICs is hindered by poor fabrication tolerances. In this work we present a fully passive, highly fabrication tolerant polarization beam splitter, based on an asymmetrical Mach-Zehnder interferometer (MZI) with a Si/SiO_2 Periodic Layer Structure (PLS) on top of one of its arms. By engineering the birefringence of the PLS we are able to design the MZI arms so that sensitivities to the most critical fabrication errors are greatly reduced. Our PBS design tolerates waveguide width variations of 400nm maintaining a polarization extinction ratio better than 13dB in the complete C-Band.

OCIS codes: (230.5440) Polarization-selective devices; (230.3120) Integrated optics devices.

References and links

1. T. Barwicz, M. R. Watts, P. A. Popovic, P. T. Rakich, L. Socci, F. X. Kartner, E. P. Ippen, and H. I. Smith, "Polarization-transparent microphotonic devices in the strong confinement limit," Nat. Photonics **1**, 57–60 (2007).
2. E. Ip, A. P. T. Lau, D. J. F. Barros, and J. M. Kahn, "Coherent detection in optical fiber systems," Opt. Express **16**, 753–791 (2007).
3. W. Yuan, K. Kojima, B. Wang, T. Koike-Akino, K. Parsons, S. Nishikawa, and E. Yagyu, "Mode-evolution-based polarization rotator-splitter design via simple fabrication process," Opt. Express **20**, 10163–10169 (2012).
4. J. M. Hong, H. H. Ryu, S. R. Park, J. W. Jeong, S. G. Lee, E.-H. Lee, S.-G. Park, D. Woo, S. Kim, and B.-H. O, "Design and fabrication of a significantly shortened multimode interference coupler for polarization splitter application," IEEE Photon. Technol. Lett. **15**, 72–74 (2003).
5. L. M. Augustin, J. J. G. M. van der Tol, R. Hanfoug, W. J. M. de Laat, M. J. E. van de Moosdijk, P. W. L. van Dijk, Y.-S. Oei, and M. K. Smit, "A single etch-step fabrication-tolerant polarization splitter," J. Lightwave Technol. **25**, 740–746 (2007).
6. D. Dai, Z. Wang, J. Peters, and J. E. Bowers, "Compact polarization beam splitter using an asymmetrical mach–zehnder interferometer based on silicon-on-insulator waveguides," IEEE Photon. Technol. Lett. **24**, 673–675 (2012).
7. L. B. Soldano, A. I. de Vreede, M. K. Smit, B. H. Verbeek, E. G. Metaal, and F. H. Green, "Mach-zehnder interferometer polarization splitter in ingaasp/inp," IEEE Photon. Technol. Lett. **6**, 402–405 (1994).
8. J. J. G. M Vand der Tol, M. Felicetti, and M. K. Smit, "Increasing Tolerance in Passive Integrated Optical Polarization Converters," J. Lightw. Technol. **30**, 2884–2889 (2012).

#188260 - $15.00 USD Received 8 Apr 2013; revised 8 May 2013; accepted 23 May 2013; published 6 Jun 2013

9. C. Alonso-Ramos, S. Romero-García, A. Ortega-Moñux, I. Molina-Fernández, R. Zhang, H. G. Bach, and M. Schell, "Polarization rotator for InP rib waveguide," Opt. Lett. **37**, 335–337 (2012).
10. C. R. Doerr, L. Zhang, P. J. Winzer, N. Weimann, V. Houtsma, T. Hu, N. J. Sauer, L. L. Buhl, D. T. Neilson, S. Chandrasekhar, and Y. K. Chen, "Monolithic inp dual-polarization and dual-quadrature coherent receiver," IEEE Photon. Technol. Lett. **23**, 694–696 (2011).
11. D. Dai, Z. Wang, and J. E. Bowers, "Considerations for the design of asymmetrical mach–zehnder interferometers used as polarization beam splitters on a submicrometer silicon-on-insulator platform," J. Lightwave Technol. **29**, 1808–1817 (2011).
12. C. Alonso-Ramos, R. Halir, A. Ortega-Moñux, P. Cheben, L. Vivien, I. Molina-Fernández, D. Marris-Morini, S. Janz, D.-X. Xu, and J. Schmid, "Highly tolerant tunable waveguide polarization rotator scheme," Opt. Lett. **37**, 3534–3536 (2012).
13. K. Kojima, W. Yuan, B. Wang, T. Koike-Akino, K. Parsons, S. Nishikawa, and E. Yagyu, "An mmi-based polarization splitter using patterned metal and tilted joint," Opt. Express **20**, B371–B376 (2012).
14. B. Lahiri, R. Dylewicz, R. M. D. L. Rue, and N. P. Johnson, "Impact of titanium adhesion layers on the response of arrays of metallic split-ring resonators (srrs)," Opt. Express **18**, 11202–11208 (2010).
15. C. Yao, H.-G. Bach, R. Zhang, G. Zhou, J. H. Choi, C. Jiang, and R. Kunkel, "An ultracompact multimode interference wavelength splitter employing asymmetrical multi-section structures," Opt. Express **20**, 18248–18253 (2012).
16. L. B. Soldano and E. C. M. Pennings, "Optical multi-mode interference devices based on self-imaging: principles and applications," J. Lightwave Technol. **13**, 615–627 (1995).
17. R. Halir, A. Ortega-Monux, I. Molina-Fernández, J. G. Wangüemert-Pérez, P. Cheben, D.-X. Xu, B. Lamontagne, and S. Janz, "Compact high performance multi-mode interference couplers in silicon-on-insulator," IEEE Photon. Technol. Lett. **21**, 1600–1602 (2009).
18. S. M. Rytov, "Electromagnetic properties of a finely stratified medium," Sov. Phy. JETP **2**,466 (1956).
19. D. Poitras, J. A. Dobrowolski, T. Cassidy, and S. Moisa, "Ion-beam etching for the precise manufacture of optical coatings," Appl. Opt. **42**, 4037–4044 (2003).
20. P. Runge and R. Zhang, "Deposition of Periodic Layer Structures," Private Communication.

1. Introduction

Polarization management in photonic integrated circuits (PICs) is becoming of increasing importance, both to provide polarization transparency [1], and to enable polarization multiplexing in coherent communication systems [2]. Integrated PBS are key devices to realize such on chip polarization control. The principle of operation of integrated PBSs is generally based either on modal evolution [3] or interferometry. The latter include multimode interference couplers (MMI) [4], directional couplers (DC) [5], and Mach-Zehnder interferometers (MZI) [6,7]. PBSs based on DCs and MZIs are often the preferred solution as they provide the smallest footprints among the different alternatives.

However, the PBSs designs presented to date lack, to the best of our knowledge, the robustness required for satisfactory fabrication yields. This sensitivity to fabrication errors also affects other polarization handling devices, such as polarization rotators [8, 9]. To overcome the limited fabrication tolerances of the available designs, structures with active control that can compensate for fabrication variations are commonly used [10–12]. The most fabrication tolerant, fully passive PBS so far was proposed in [5]. It is based on a tapered DC and exhibits a total width tolerance of 100nm. Recently another PBS considered to be particularly tolerant to fabrication errors was presented by Kojima *et al.* [13]. The structure achieves polarization splitting by using a gold patch that introduces a phase shift between the TE and TM polarizations. However, it is well known that gold cannot be deposited without an adhesive layer of platinum/titanium. This layer needs to be considered during the simulation stage and introduces polarization dependent losses that may require redesign to mitigate its effects [14].

In this work we propose a fully passive MZI based PBS with a periodic layer structure (PLS) on top of one of the MZI arms. The PLS allows us to design the waveguide birefringence without using metals, so that polarization dependent losses are negligible. Besides, this approach overcomes the main limitation of asymmetric MZI based PBSs, namely the high sensitivity to width errors in the width of the MZI arms [10, 11]. As a result, no active tuning

#188260 - $15.00 USD Received 8 Apr 2013; revised 8 May 2013; accepted 23 May 2013; published 6 Jun 2013

is required. Fully-etched InP/InGaAsP ridge waveguides with 1045nm etch-depth have been used in the design, thus maintaining compatibility with previously proposed devices [15]. The device exhibits width tolerances up to 400nm for a polarization extinction ratio of 13dB in the C-Band, thereby providing a four-fold improvement over state-of-the-art passive PBSs.

2. Principle of operation

The structure of a MZI based PBS is shown schematically in Fig. 1. It comprises two MMI couplers interconnected by two waveguide arms of length L. The first MMI acts as a power splitter whereas the second MMI acts as a $3\text{dB}/90^\circ$ coupler. The design and fabrication of MMI structures has been widely discussed in literature (see, for instance [16, 17]). Since MMIs are furthermore known to exhibit relaxed fabrication tolerances, hereafter we will focus solely on the design of the interconnecting waveguides.

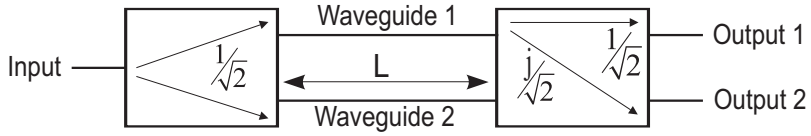

Fig. 1. Schematic of a generic MZI-PBS.

Referring to Fig. 1, the normalized output powers of an MZI based PBS are given by [11]:

$$\begin{aligned} P_1 &= 0.5\left[1+\sin\left(\left(\beta_2-\beta_1\right)L\right)\right] \\ P_2 &= 0.5\left[1-\sin\left(\left(\beta_2-\beta_1\right)L\right)\right] \end{aligned} \tag{1}$$

where β_1 and β_2 are the propagation constants of the fundamental TE/TM mode of waveguides 1 and 2. In order to work as a PBS the device must direct all power carried by the TE polarization to output 1, and all power carried by the TM polarization to output 2, i.e. $P_1^{\text{TE}}=1$, $P_1^{\text{TM}}=0$, $P_2^{\text{TE}}=0$ and $P_1^{\text{TM}}=1$. The polarization extinction ratio (ER) of the PBS is then defined as the minimum between $\text{ER}_{\text{TE}}=P_1^{\text{TE}}/P_1^{\text{TM}}$, $\text{ER}_{\text{TM}}=P_2^{\text{TM}}/P_2^{\text{TE}}$. For perfect polarization splitting, the propagation constants (β) of the fundamental TE and TM modes of the waveguide arms must then fulfill:

$$\begin{aligned} (\beta_2^{\text{TE}}-\beta_1^{\text{TE}})L &= \tfrac{\pi}{2} \\ (\beta_2^{\text{TM}}-\beta_1^{\text{TM}})L &= -\tfrac{\pi}{2} \end{aligned} \tag{2}$$

Assuming that the previous conditions are simultaneously satisfied [11], the length of the arms (L) can be written as a function of waveguide birefringences:

$$L=\frac{\pi}{(\beta_2^{\text{TE}}-\beta_2^{\text{TM}})-(\beta_1^{\text{TE}}-\beta_1^{\text{TM}})}=\frac{\pi}{\Delta\beta_2-\Delta\beta_1} \tag{3}$$

where $\Delta\beta_1$ and $\Delta\beta_2$ is the modal birefringence of waveguides 1 and 2 respectively.

To model the effect of fabrication tolerances, we expand the propagation constants in Eq. (2) to first order, i.e. $\beta=\beta_{\text{nominal}}+\frac{\partial\beta}{\partial p}\Delta p$, where Δp is a variation in one of the waveguide parameters (waveguide width, thickness) and $\frac{\partial\beta}{\partial p}$ is the sensitivity of the propagation constant to changes in that waveguide parameter. By requiring Eq. (2) to hold for non-zero Δp, we find:

$$\begin{aligned} \frac{\partial\beta_2^{\text{TE}}}{\partial p}-\frac{\partial\beta_1^{\text{TE}}}{\partial p}&=0 \\ \frac{\partial\beta_2^{\text{TM}}}{\partial p}-\frac{\partial\beta_1^{\text{TM}}}{\partial p}&=0 \end{aligned}, \tag{4}$$

#188260 - $15.00 USD Received 8 Apr 2013; revised 8 May 2013; accepted 23 May 2013; published 6 Jun 2013

i.e. for relaxed fabrication tolerances, the sensitivities of the propagation constants in the upper and lower arm should be identical for both polarizations.

From Eq. (3) it can be seen that in order to achieve a compact footprint the modal birefringences of the waveguides should be very different ($\Delta\beta_2 \gg \Delta\beta_1$). In the conventional design approach, this is achieved by choosing two waveguides with very different widths, as depicted in Fig. 2(a). However, the condition for relaxed fabrication tolerances (4) cannot be met with this approach because in the wide waveguide the sensitivity of the propagation constants to width changes is $\sim 0.005\text{rad}/\mu\text{m}^2$, whereas in the narrow waveguide this sensitivity is $\sim 0.1\text{rad}/\mu\text{m}^2$, i.e. 20 times higher.

3. Design method for relaxed tolerances

In order to achieve both a compact footprint and relaxed tolerances we propose to deposit a PLS on top of one of the MZI arms [Fig. 2(b)]. The PLS behaves as an artificial birefringent material [18], thereby allowing us to design the waveguide birefringence while maintaining relaxed fabrication tolerances. The PLS comprises thin layers of Silicon (Si) and Silicon Dioxide (SiO_2), as shown in Fig. 2(b). This structure can be deposited through a sputtering process, which is compatible with standard fabrication flows. Sputtering is a well-known deposition technique and has a precision of $\sim \pm 1$nm in the thicknesses of the layers [19]. Due to technological reasons the total number of layers in the PLS is set to 20 and the sum of the thicknesses of a Silicon layer. The ratio between the thickness of the layers on the sidewalls to the thickness of the horizontal layers is 0.5 [20].

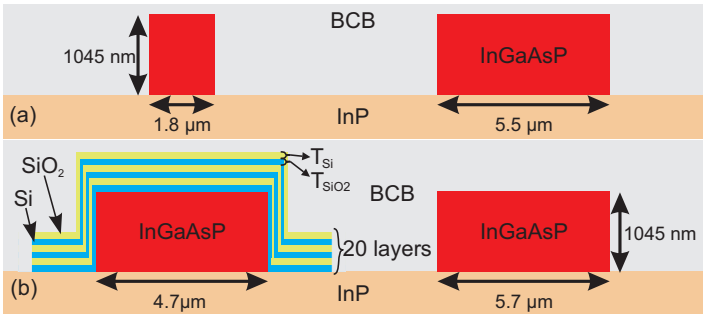

Fig. 2. Cross-sectional dimensions of the MZI-PBS arms, in (a) the conventional approach, and (b) the PLS approach.

The design of the waveguides is carried out using a variable separation procedure, consisting of two steps. First the PLS is designed to achieve the desired birefringence considering only the vertical dimensions, i.e. using slab waveguides. Once the PLS is fixed, the waveguide widths are calculated.

Designing the PLS requires finding the thickness of the Silicon (T_{Si}) and the Silicon Dioxide (T_{SiO_2}) layers. In this step, waveguides are considered slabs in the horizontal direction, so the birefringence of the arms can be calculated analytically for a large number of pairs of T_{Si} and T_{SiO_2} with reduced computational effort. Applying these calculations to Eqs. (1)–(3) an estimation of the length of the arms and the ER can be obtained for each combination of T_{Si} and T_{SiO_2}. Using the obtained ER the tolerance to thickness errors is calculated at the central wavelength (1550nm). The results of this analysis are presented in Fig. 3, where length estimation [Fig. 3(a)] and tolerance to thickness error for an ER greater than 13dB [Fig. 3(b)] are shown as a function of T_{Si} and T_{SiO_2}. From Fig. 3(a) MZI arms are found to be shortest when the silicon layers are $70-80$nm thick and the silicon dioxide layers are $20-30$nm

#188260 - $15.00 USD Received 8 Apr 2013; revised 8 May 2013; accepted 23 May 2013; published 6 Jun 2013

thick. However the best tolerances to thickness errors are obtained when T_{Si} varies between $60-70$nm and T_{SiO_2} varies between $30-40$nm [Fig. 3(b)]. It is important to remember that $T_{Si}+T_{SiO_2}$ should be thinner than 100nm. Finally, $T_{Si}=65$nm and $T_{SiO_2}=35$nm have been chosen to maximize tolerances to thickness errors (>2nm) while ensuring MZI arms of reasonable length ($\sim 300\mu$m).

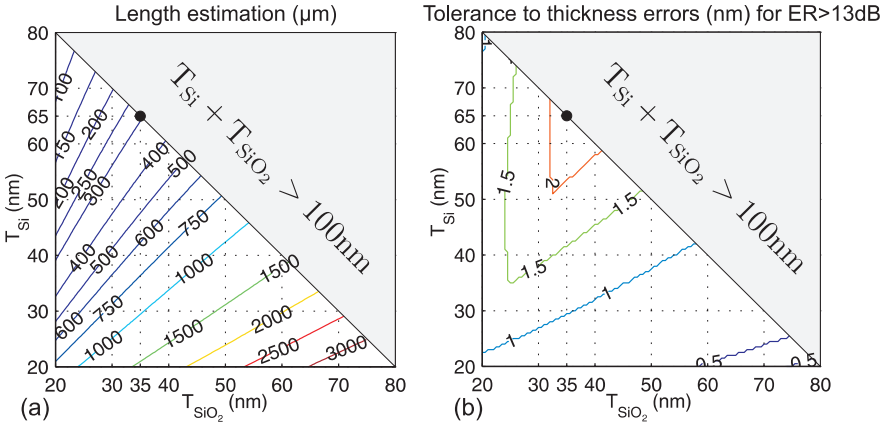

Fig. 3. (a) Estimation of the length of the arms as a function of Si/SiO_2 layer thicknesses. (b) Minimum thickness tolerances as a function of Si/SiO_2 layer thicknesses for a wavelength of 1550nm. The design point is shown with a dot.

Once the PLS is designed, waveguide widths are calculated following the method proposed in [11]. Special care is taken in choosing the waveguide widths to ensure that sensitivities to width variations are similar in both waveguides, so that relaxed width tolerances are achieved. In the design presented here the widths are 4.7μm for the PLS waveguide and 5.7μm for the conventional waveguide. In this case the sensitivity to width variations in the PLS waveguide ($0.006\text{rad}/\mu\text{m}^2$) is similar to the waveguide without PLS ($0.004\text{rad}/\mu\text{m}^2$). Since the fundamental modes are laterally well confined in the InP core of the PLS waveguide the sidewall-to-horizontal thickness ratio has little impact on device performance. In fact, this ratio can vary within $0.35-0.65$ maintaining an extinction ratio better than 30dB. The resulting length of the MZI arms is 311.5μm.

The complete PBS requires several additional structures, as shown in Fig. 4. The layout incorporates s-bends and tapers which are necessary to adapt the different waveguides cross-sections. The tapers are identical in both arms, so that phase shifts and losses introduced by the tapers cancels out. Since the PLS cladding significantly changes the waveguide geometry, it is crucial to design an adiabatic transition to the unclad waveguides. Here we propose the use of a 25μm long wedge form taper which relaxes mask alignment tolerances. The complete PBS structure is 1.5mm long and has insertion losses below 0.5dB.

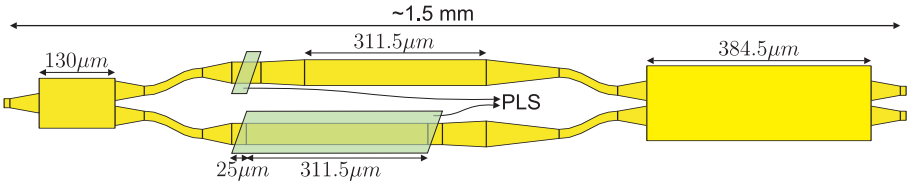

Fig. 4. Layout of the proposed PBS.

#188260 - $15.00 USD Received 8 Apr 2013; revised 8 May 2013; accepted 23 May 2013; published 6 Jun 2013

4. Simulation results

To assess the performance and tolerances of our design, all structures were simulated using the 3D Full Vectorial software FIMMWAVE varying the width of MMIs and MZI arms in $\pm$200nm, and the PLS layer thicknesses (ΔT) in $\pm$1nm. For comparison a traditional PBS based on waveguides of different widths, as shown in Fig. 2(a), was also designed and optimized; the length of the MZI arms in this case is 260.5μm. The performance of both designs is compared in Fig. 5, which shows the minimum ER in the C-Band (1530nm - 1570nm) as a function of waveguide width deviation. The conventional PBS has a total width tolerance of approximately 25nm for an ER above 13dB, while the PLS based PBS proposed in this work has a total width tolerance of over 400nm. The PBS presented in this work achieves a significant increase of fabrication tolerances with a shorter device over state-of-the-art PBSs in terms of fabrication tolerances. The effect of variations in the thickness of the PLS layers is also shown in Fig. 5. Note that even for the maximum variations of $\pm$1nm expected from the sputtering process the ER exceeds 13dB in the complete C-Band.

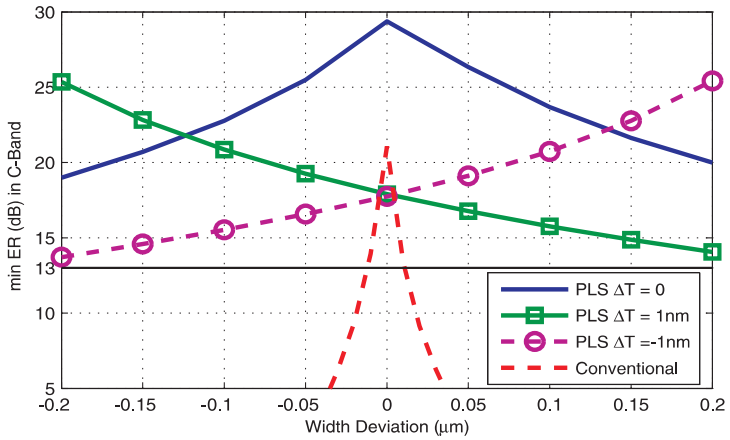

Fig. 5. Minimum ER in the C-Band as a function of the width error for a conventional PBS and our design. The ER for different errors in the thickness of the PLS layers is also shown.

5. Conclusion

In this work a fully passive, Mach-Zehnder based PBS in III-V technology with relaxed width tolerances of 400nm is presented. These tolerances are achieved by making use of a birefringent PLS, and by designing the waveguides so that sensitivity to widths variations is minimized. A method for efficiently designing this kind of PBS is also presented. The same technique can be applied for designing PBSs in other technologies like silicon-on-insulator. We expect this device to facilitate the practical realization of polarization diversity circuits such as coherent receivers with polarization multiplexing. Our PLS approach furthermore offers interesting prospectives for the design of other polarization management devices.

Acknowledgments

The authors want to acknowledge the funding from the Spanish Ministry of Science (project TEC2009-10152) and the European Mirthe project (FP7-2010-257980).

#188260 - $15.00 USD Received 8 Apr 2013; revised 8 May 2013; accepted 23 May 2013; published 6 Jun 2013